

Traffic of interacting ribosomes: effects of single-machine mechano-chemistry on protein synthesis

Aakash Basu¹ and Debashish Chowdhury*¹

¹*Department of Physics, Indian Institute of Technology, Kanpur 208016, India.*

(Dated: May 25, 2019)

Many *ribosomes* simultaneously move on the same messenger RNA (mRNA), each synthesizing a protein. Earlier models of ribosome traffic represent each ribosome by a “self-propelled particle” and capture the dynamics by an extension of the totally asymmetric simple exclusion process. In contrast, here we develop a “unified” theoretical model that not only incorporates the *mutual exclusions* of the interacting ribosomes, but also describes explicitly the mechano-chemistry of each of these individual cyclic machines during protein synthesis. Using a combination of analytical and numerical techniques of non-equilibrium statistical mechanics, we analyze this model and illustrate its power by making experimentally testable predictions on the rate of protein synthesis and the density profile of the ribosomes on some mRNAs in *E-Coli*.

Translation, the process of synthesis of proteins by decoding genetic information stored in the mRNA, is carried out by *ribosomes*, which are among the largest and most complex macromolecular machines within the cell [1]. Fundamental understanding of the interplay of the biochemical reactions and mechanical movements of ribosomes will not only provide deep insight into the mechanisms of regulation and control of protein synthesis, but also find biomedical applications as ribosome is the target of many antibiotics [2].

Most often many ribosomes move simultaneously on the same mRNA strand while each synthesises a protein. The inter-ribosome interactions cannot be ignored except at extremely low densities. In all the earlier models of collective traffic-like movements of ribosomes [3, 4, 5, 6, 7, 8, 9], the entire ribosome is modelled as a single “self-propelled particle” ignoring its molecular composition and architecture. Moreover, in these models the inter-ribosome interactions are captured through hard-core mutual exclusion and the dynamics of the system is formulated in terms of rules that are essentially straightforward extensions of the totally asymmetric simple exclusion process (TASEP) [10].

In reality, the mechanical movement of each ribosome is coupled to its biochemical cycle. The earlier TASEP-like models successfully explain some of the collective properties of ribosome traffic but fail to account for those aspects of spatio-temporal organization that depend on detailed mechano-chemical cycle of each ribosome. In this letter we develop a “unified” model that not only incorporates the hard-core mutual exclusion of the interacting ribosomes, but also captures explicitly the essential steps in the biochemical cycle of each ribosome, including GTP (guanine triphosphate) hydrolysis, and couples it to its mechanical movement during protein synthesis. Consequently, in the low-density limit, our model accounts

for the protein synthesis by a single isolated ribosome while at higher densities the same model predicts not only the rate of protein synthesis but also the collective density profile of the ribosomes on the mRNA strand.

We represent the mRNA chain, consisting of L codons, by a one-dimensional lattice of length $L + \ell - 1$ where each of the first L sites from the left represents a single codon (i.e., a triplet of nucleotides). We label the sites of the lattice by the integer i ; the sites $i = 1$ and $i = L$ represent the start codon and the stop codon, respectively.

The small sub-unit of the ribosome, which is known to bind with the mRNA, is represented by an *extended particle* of length ℓ (in the units of the size of a codon), as shown in fig.1(a) ($\ell = 12$ for all results reported here). [4, 5, 6, 7, 8, 9], Thus, the small subunit of each ribosome covers ℓ codons at a time (see fig.1(b)). According to our convention, the *position* of such a ribosome on the mRNA strand will be given by the position of the lattice site covered by the *left* edge of its smaller subunit. Each ribosome moves forward by only one site in each step as it must translate successive codons one by one. The mutual interactions of the ribosomes translocating on the same mRNA is taken into account by imposing the constraint of mutual exclusion.

The process of translation itself can be divided into three main stages: (a) *initiation*, (b) *elongation*, and (c) *termination*. Since our model is *not* intended to describe initiation and termination in detail, we represent initiation and termination by the two parameters α and β , respectively (see fig.1(b)). If the first ℓ sites on the mRNA are vacant, this group of sites is allowed to be covered by a ribosome, from the pool of unbound ribosomes, with probability α in the time interval Δt (in all our numerical calculations we take $\Delta t = 0.001$ s). Similarly, if the rightmost ℓ sites of the mRNA lattice are covered by a ribosome, i.e., the ribosome is bound to the L -th codon, the ribosome gets detached from the mRNA with probability β in the time interval Δt . Moreover, since α is the probability of attachment in time Δt , the probability of attachment per unit time (which we call ω_α) is the

*Corresponding author: debch@iitk.ac.in

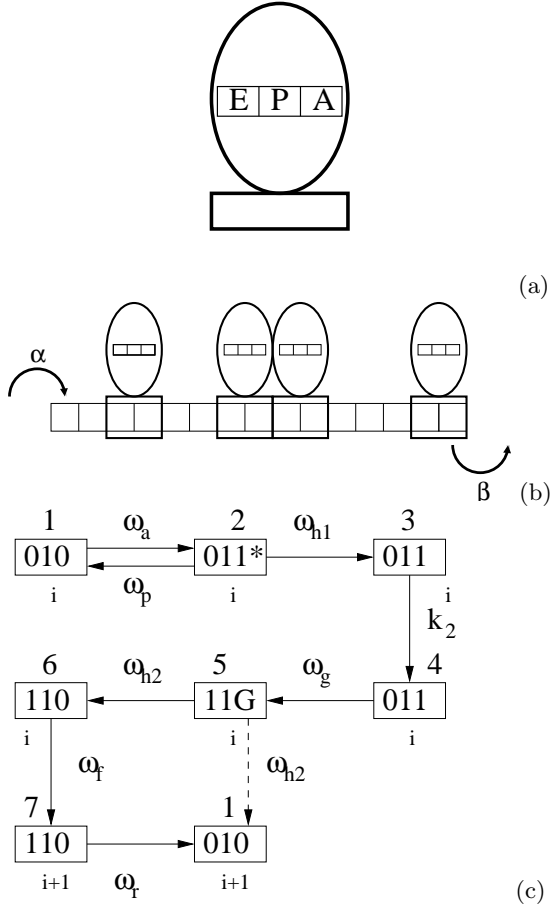


FIG. 1: (a) The model ribosome is shown schematically with the three binding sites (E, P, A) on its larger subunit. (b) The mRNA is represented by a one-dimensional lattice each site of which corresponds to a distinct codon; the smaller subunit of the ribosome (the rectangle in (a)) can cover simultaneously ℓ codons ($\ell = 2$ in this figure). The parameters α and β capture the effective rates of initiation and termination of translation. (c) The biochemical cycle of a single ribosome during the elongation stage. Each box represents a distinct state of the ribosome. The index below the box labels the codon on the m-RNA with which the smaller subunit of the ribosome binds. The number above the box labels the biochemical state of the ribosome. Within each box, 1(0) represents presence (absence) of tRNA on binding sites E, P, A. 1* is a EF-Tu bound tRNA and G is a EF-G GTPase. The symbols accompanied by the arrows define the rate constants for the corresponding transitions. The dashed arrow represents the approximate pathway we have considered in our model.

solution of the equation $\alpha = 1 - e^{-\omega_\alpha \times \Delta t}$.

To our knowledge, all the earlier models of ribosome traffic on mRNA [3, 4, 5, 6, 7, 8, 9], describe elongation also by a single parameter, namely, the rate q of hopping of a ribosome from one codon to the next. In contrast, we model the chemo-mechanics of elongation in detail. We first identify *seven* distinct states of the ribosome in each such cycle as shown schematically in fig.1(c). How-

ever, in setting up the rate equations below, we treat the entire transition $5 \rightarrow 6 \rightarrow 7 \rightarrow 1$ as, effectively, a single step transition from 5 to 1, with rate constant ω_{h2} . Thus, throughout this paper we work with a simplified model where each biochemical cycle during the elongation process consists of *five* distinct states.

The modelling strategy adopted here for incorporating biochemical cycle of ribosomes is similar to that followed in the recent work [11] on single-headed kinesin motors KIF1A. However, the implementation of the strategy is more difficult here not only because of the higher complexity of composition, architecture and mechanochemical processes of the ribosomal machinery and but also because of the *heterogeneity* of the mRNA track [12].

Let $P_\mu(i)$ be the probability of finding a ribosome at site i , in the chemical state μ . Then, $P(i) = \sum_{\mu=1}^5 P_\mu(i)$, is the probability of finding a ribosome at site i , irrespective of its chemical state. Moreover, if a site is *not* covered by any part of any ribosome, we'll say that the site is occupied by a "hole". Furthermore, by the symbol $Q(i|j)$ we denote the conditional probability that, given a ribosome at site i , there is a hole at the site j . The master equations for the probabilities $P_\mu(i)$ are given by

$$\begin{aligned} \frac{dP_1(i)}{dt} &= \omega_{h2}P_5(i-1)Q(i-1|i-1+\ell) \\ &\quad + \omega_p P_2(i) - \omega_a P_1(i) \end{aligned} \quad (1)$$

$$(i \neq 1)$$

$$\frac{dP_2(i)}{dt} = \omega_a P_1(i) - (\omega_p + \omega_{h1})P_2(i) \quad (2)$$

$$\frac{dP_3(i)}{dt} = \omega_{h1}P_2(i) - k_2 P_3(i) \quad (3)$$

$$\frac{dP_4(i)}{dt} = k_2 P_3(i) - \omega_g P_4(i) \quad (4)$$

$$\begin{aligned} \frac{dP_5(i)}{dt} &= \omega_g P_4(i) - \omega_{h2}P_5(i)Q(i|i+\ell) \end{aligned} \quad (5)$$

$$(i \neq L)$$

However, the equations for $P_1(1)$ and $P_5(L)$ have the special forms

$$\frac{dP_1(1)}{dt} = \omega_\alpha \left(1 - \sum_{s=1}^{\ell} P(s)\right) + \omega_p P_2(1) - \omega_a P_1(1) \quad (6)$$

$$\frac{dP_5(L)}{dt} = \omega_g P_4(L) - \beta P_5(L). \quad (7)$$

Because of the finite length of the codon sequence between the start and stop codons, the open boundary conditions (OBC) are more realistic than the periodic boundary conditions (PBC). However, we begin with a calculation of the flux of the ribosomes in the steady-state by

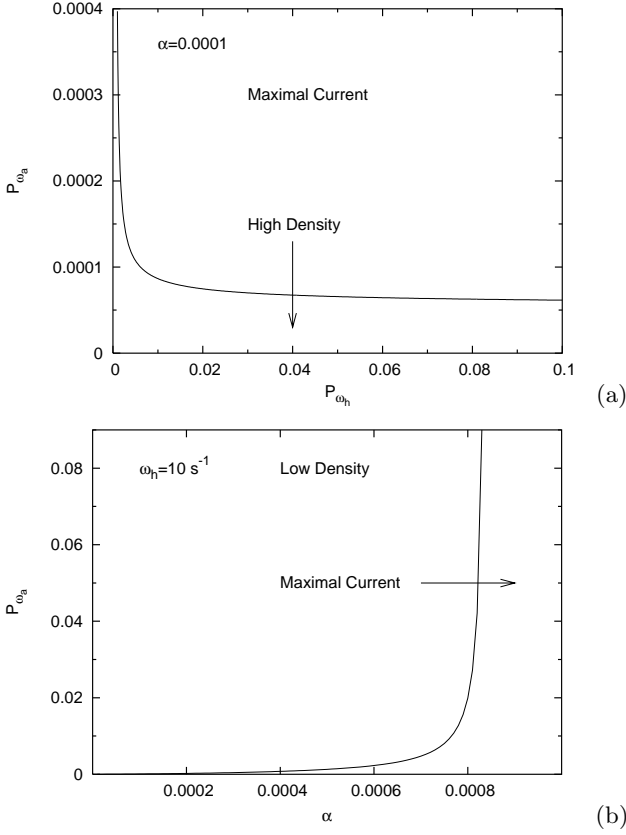


FIG. 2: Phase diagram in (a) $P_{\omega_h} - P_{\omega_a}$ plane and (b) $\alpha - P_{\omega_a}$ plane.

imposing PBC as the results for this artificial situation are required for a derivation of the dynamical phase diagram of the system under OBC. Under PBC, $P_\mu(i)$ for all i are governed by the equations (1)-(5). Moreover, under the PBC, only four of the five equations (1)-(5) are independent because $P(i) = \sum_{\mu=1}^5 P_\mu(i) = N/L = \rho$ where ρ , the number density of the ribosomes, is a constant independent of time; therefore, we do not need to consider equation (1) for $P_1(i)$ explicitly. In the steady state, all time derivatives vanish and because of the translational invariance of this state under PBC, the index i can be dropped. It is straightforward to show [13] that, for PBC,

$$Q(i|i+\ell) = \frac{L - N\ell}{L + N - N\ell - 1}. \quad (8)$$

Therefore, under the PBC, equations (2-5) can be solved, using (8), to obtain

$$P_5 = \frac{P}{1 + \frac{\omega_{h2}(L-N\ell)}{L+N-N\ell-1} \left[\frac{1}{k_{eff}} \right]} \quad (9)$$

where

$$\frac{1}{k_{eff}} = \frac{1}{\omega_g} + \frac{1}{k_2} + \frac{1}{\omega_{h1}} + \frac{1}{\omega_a} + \frac{\omega_p}{\omega_a \omega_{h1}} \quad (10)$$

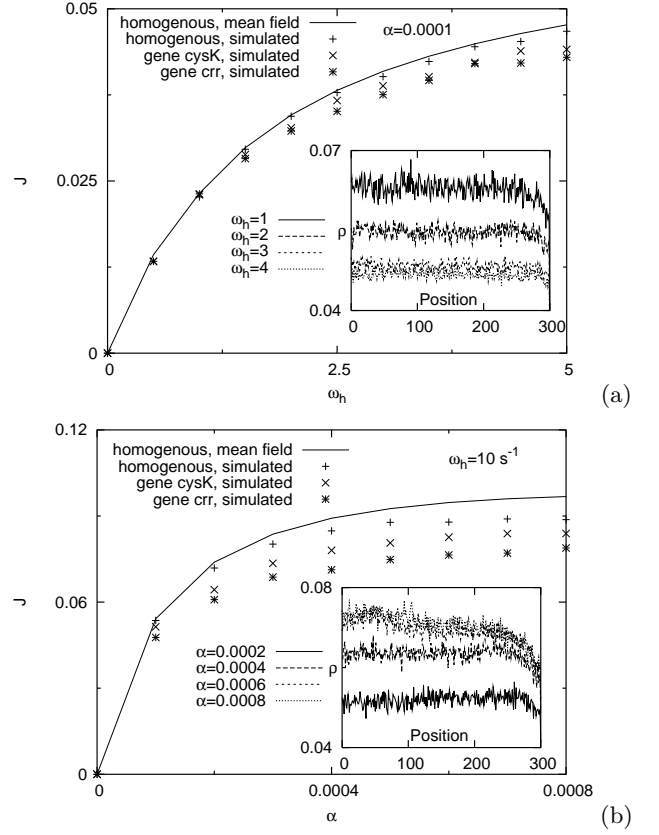


FIG. 3: Flux of ribosomes plotted against (a) ω_h and (b) α for the genes *crr* (170 codons) and *cysK* (324 codons) of *Escherichia coli* K-12 strain MG1655, as well as the corresponding curve for a homogenous mRNA strand of 300 codons. The insets show the average density profiles on a hypothetical *homogeneous* mRNA track for four different values of (a) ω_h and (b) α .

The flux of ribosomes J , under PBC, obtained from $J = \omega_{h2} P_5 Q(i|i+\ell)$, is

$$J = \frac{\omega_{h2} \rho (1 - \rho \ell)}{(1 + \rho - \rho \ell) + \Omega_{h2} (1 - \rho \ell)} \quad (11)$$

where $\Omega_{h2} = \omega_{h2}/k_{eff}$. The rate of protein synthesis by a single ribosome is ℓJ . This mean-field estimate is a reasonably good approximation to the data obtained by direct computer simulations [13].

It can be shown [13] that, for OBC,

$$Q(i|i+\ell) = \frac{1 - \sum_{s=1}^{\ell} P(i+s)}{1 - \sum_{s=1}^{\ell} P(i+s) + P(i+\ell)} \quad (12)$$

and the corresponding flux can be obtained from

$$J = \omega_a \left(1 - \sum_{s=0}^{\ell} P_s \right) \quad (13)$$

Motivated by the recent measurements [14, 15] of the number of bound ribosomes on the mRNA, we have computed the detailed concentration profiles of the ribosomes

and also drawn the phase diagrams in the spirit of the similar plots of non-equilibrium dynamical phases of totally asymmetric simple exclusion process [10].

The probabilities α and β of initiation and termination are incorporated into the model by connecting the ends of the mRNA strand to two hypothetical reservoirs with appropriate densities ρ_- and ρ_+ , respectively [5]. The extremum principle [10, 16] then relates the flux j in the open system to the flux $J(\rho)$ for a closed periodic system with the same dynamics:

$$j = \begin{cases} \max J(\rho) & \text{if } \rho_- > \rho > \rho_+ \\ \min J(\rho) & \text{if } \rho_- < \rho < \rho_+ \end{cases}$$

For systems with a single maximum in the function $J(\rho)$, at $\rho = \rho_*$, such as equation (11), the maximal current phase sets in when $\rho_- > \rho_* > \rho_+$. By differentiating equation (11), we find [13]

$$\rho_* = \frac{-\ell(1 + \Omega_{h2}) + \sqrt{\ell(1 + \Omega_{h2})}}{\ell(1 - \ell - \Omega_{h2}\ell)} \quad (14)$$

It can also be shown that [13]

$$\rho_- = \frac{\alpha(1 - \frac{\ell}{L})(1 + \Omega_{h2})}{P_{\omega_h} - \alpha(1 + \Omega_{h2})(1 - \ell)} \quad (15)$$

where P_{ω_h} is the probability of hydrolysis in the time Δt , and that $\rho_+ = 0$. Similarly, the probability of attachment of a *aa-tRNA* in time Δt is denoted by P_{ω_a} . Thus, the phase boundaries between the various phases have been obtained by solving the equation

$$\rho_-(\alpha, \omega_a, \omega_{h1}, \omega_{h2}) = \rho_*(\alpha, \omega_a, \omega_{h1}, \omega_{h2}) \quad (16)$$

numerically, and two typical phase diagrams have been plotted in figs.2(a) and (b) assuming [17, 18] $\omega_{h1} = \omega_{h2} = \omega_h$.

We focus on genes of *Escherichia coli* K-12 strain MG1655 [19]. We directly simulate the system by assuming that the site dependent transition rate ω_a is proportional to the percentage availability of the corresponding aa-tRNA for that codon, in the E Coli cell [20, 21]. In figure (3), we see how the current increases as ω_h (in (a)) and α (in (b)) increases and gradually saturates; the saturation value of the current is numerically equal to the maximum current obtained in the corresponding case with PBC [13]. Simultaneously, the average density of the ribosomes decreases in (a) (and increases in (b)) as the parameter ω_h in (a) (and α in (b)) increases, and gradually saturates. These observations are consistent with the scenario of phase transition from the low density phase to the maximal current phase, as predicted by the extremal current hypothesis. Moreover, the lower flux observed for real genes, as compared to that for homogeneous mRNA, is caused by the codon specificity of the available tRNA molecules.

In this letter we have developed a ‘‘unified’’ theoretical model for protein synthesis by mutually interacting ribosomes following the master equation approach of non-equilibrium statistical mechanics. We have computed (i) the rate of protein synthesis in real time and (ii) density profile of the ribosomes on a given mRNA, and studied their dependences on the rates of various *mechanochemical* processes in each ribosome. We have illustrated the use of our model by applying these to two genes of *E-Coli* and making theoretical predictions which, we hope, will motivate new *quantitative* measurements.

-
- [1] A.S. Spirin, FEBS Lett. **514**, 2 (2002).
[2] T. Hermann, Curr. Op. in str. biol. **15**, 355 (2005).
[3] C.T. MacDonald and J.H. Gibbs, Biopolymers **7**, 707 (1969).
[4] G. Iakatos and T. Chou, J. Phys. A **36**, 2027 (2003).
[5] L.B. Shaw, R.K.P. Zia and K.H. Lee, Phys. Rev. E **68**, 021910 (2003).
[6] L.B. Shaw, J.P. Sethna and K.H. Lee, Phys. Rev. E **70**, 021901 (2004).
[7] L.B. Shaw, A.B. Kolomeisky and K.H. Lee, J. Phys. A **37**, 2105 (2004).
[8] T. Chou, Biophys. J., **85**, 755 (2003).
[9] T. Chou and G. Iakatos, Phys. Rev. Lett. **93**, 198101 (2004).
[10] G. Schütz, Phase Transitions and Critical Phenomena, vol. 19 (Acad. Press, 2001).
[11] K. Nishinari, Y. Okada, A. Schadschneider and D. Chowdhury, Phys. Rev. Lett. **95**, 118101 (2005).
[12] Y. Kafri and D.R. Nelson, J. Phys. Cond. Matt. **17**, S3871 (2005).
[13] A. Basu and D. Chowdhury, to be published.
[14] Y. Arava, F.E. Boas, P.O. Brown and D. Herschlag, Nucl. Acids Res. **33**, 2421 (2005).
[15] V.L. Mackay, X. Li, M.R. Flory, E. Turcott, G.L. Law, K.A. Serikawa, X.L. Xu, H. Lee, D.R. Goodlett, R. Aebersold, L.P. Zhao and D.R. Morris, Mol. cell. proteomics, **3**, 478 (2004).
[16] V. Popkov and G. Schütz, Europhys. Lett. **48**, 257 (1999).
[17] R.C. Thompson, D.B. Dix and J.F. Eccleston, J. Biol. Chem. **255**, 11088 (1980).
[18] K.M. Harrington, I.A. nazarenko, D.B. Dix, R.C. Thompson and O.C. Uhlenbeck, Biochem. **32**, 7617 (1993).
[19] see <http://www.genome.wisc.edu/sequencing/k12.htm>
[20] J. Solomovici, T. Lesnik and C. Reiss, J. Theor. Biol. **185**, 511 (1997).
[21] S.G.E. Andersson and C.G. Kurland, Microbiol. Rev. **54**, 198 (1990).